Knowledge-based Engineering and Sciences (2024), **5**, (1), 98–119
doi:10.51526/kbes.2024.5.1.98-119

RESEARCH PAPER

Optimizing 2-Nitrophenol and Chromium Adsorption from Water with Aluminium Oxide via Response Surface Methodology

Hamza A. Asmaly,[*,1] Nassereldeen Kabbashi,[*,1] Ma'an Fahmi Al-Khatib,[1] Md Zahangir Alam,[2] and N.F.M Khairuddin[3]

[1]Department of Biotechnology Engineering, International Islamic University Malaysia, Gombak, 53100 Kuala Lumpur, Malaysia
[2]Department of Chemical Engineering and Sustainability, International Islamic University Malaysia, Gombak, 53100 Kuala Lumpur, Malaysia
[3]Interdisciplinary Research Centre for Membranes and Water Security, King Fahd University of Petroleum and Minerals, Dhahran 31261, Saudi Arabia
[*]Corresponding author. Email: hamzaa@kfupm.edu.sa; nasreldin@iium.edu.my

(Received 08 March 2024; revised 20 April 2024; accepted 29 April 2024; first published online 30 April 2024)

Abstract

The study explored the efficacy of an innovative adsorbent crafted from carbon nanotubes and carbon nano fibbers integrated with aluminium oxide, in purging water solutions of both organic (2-Nitrophenol) and inorganic (Chromium III) contaminants. The study refined the aluminium impregnation method to boost the adsorption efficiency of CNAs/Al_2O_3 in removing certain pollutants. Through a central composite design (CCD) strategy, optimal adsorption conditions were determined. The most effective removal of 2-NPh (2-Nitrophenol) and Cr^{3+} (Chromium III) occurred with CNAs/Al_2O_3 at an 18% impregnation ratio, after 3 hours of ultrasonication and calcination Temperature at 300°C. This technique yielded adsorption capacities of 82.02mg/g for 2-NPh and 96.57mg/g for Cr^{3+}. The aluminium content in the adsorbents, prepared under these specified conditions, was verified, and measured using EDX (Energy Dispersive X-ray) analysis. Further, BET (Brunauer-Emmett-Teller) measurements revealed the impact of aluminium ratios on the surface area of CNAs/Al_2O_3, where an 18% aluminium ratio led to a surface area of 176 m^2/g, diminishing to 125 m^2/g and 110 m^2/g for 20% and 22% aluminium ratios, respectively. The Predicted adsorption capacity for 2-NPh was estimated at 83.154mg/g, aligning closely with the observed 82.02mg/g, while the estimate for Cr^{3+} at 97.80mg/g nearly matched the actual 96.57mg/g. A validation study evaluated the predicted adsorption capacities for both contaminants, finding that the actual capacities were 86.79mg/g for 2 – NPh and 99.79mg/g_{for} Cr^{3+}. The study noted an acceptable error margin in optimal adsorption capacity of about 4.5% for 2 – NPh and 2% for Cr^{3+}. The optimized integration of metal oxides with CNAs through impregnation significantly enhances their efficacy in removing pollutants, particularly when aluminium oxide is used to boost their capacity for purifying wastewater by extracting both organic and heavy metal contaminants.

Keywords: Chromium; 2-Nitrophenols; Aluminium oxide and Carbon Nano Adsorbent.

1. Introduction

Toxic substances, often originating from human activities, are contaminating ecosystems and posing risks to life by causing oxidative stress [1], DNA damage [2], and apoptosis [3] in living cells.

Substances like chromium (Cr) and 2-nitrophenol (2-NP) particularly are hazardous as they can travel and persist in the environment without degrading [4]. The remediation of water contaminated with these toxins can be accomplished through costly and energy-demanding methods like reverse osmosis and ion exchange [5], or less energy-intensive methods such as adsorption. Cr has been identified as a cancer potential substance as exposure to this substance is associated with multistage carcinogenesis and epigenetic alterations [6]. The transformation of Cr^{3+} to the more toxic and hazardous Cr^{4+} is a notable concern [7]. It is possible to convert Cr^{4+} back into Cr^{3+} using both biological [8] and chemical methods [9]. Regulation of Cr compounds underscores this concern, as evidenced by the EU's discharge limits, which are tailored to the specific water body affected [10]. Furthermore, 2-NP, commonly found in pharmaceuticals [11], pesticides [12], and dye products [13], pose a significant environmental concern due to their toxicity, carcinogenicity, andresistance to degradation, attributed to their unique chemical structure [14]. As a result, they are listed as EPA priority pollutants [15]. Studies in the literature have further elucidated the environmental impact of 2-NP, demonstrating their transformation into more harmful and carcinogenic byproducts through tertiary ozonation treatment [16], [17].

An adsorption method can be used to remove toxic substances and is widely favored due to its simplicity, renewability, and versatility [2], [3]. Nanoparticles, available in standalone, functionalized, modified, or substrate-incorporated forms, have been demonstrating significant promise in adsorption processes. Their high chemical activity and ability to provide customizable surface areas enhance the efficiency of adsorption [4]. Another advantage of nanoparticles is their ability to remove very low pollutant concentrations [5], can be mobilized [6], and produced in a simple and eco-friendly technique [7], [8]. Carbon nanostructures, such as carbon nanotubes (CNTs), are popular adsorbents due to their excellent surface characteristics, ease of modification, large specific surface area, simplicity, and reusability. CNTs can be functionalized both covalently [25] and non-covalently [26], similar to graphene, enhancing their suitability for various applications. CNTs and graphene belong to the same carbon family and have similar surface characteristics, but their adsorption capacities for organic pollutants differ due to their different structures and chemical properties, which allow for different organic molecule uptake mechanisms [27]. The adsorption mechanism can occur through van der Waals forces, – stacking, hydrophobic interactions, hydrogen bonding, and electrostatic interactions [28].

Metal oxides, available in nanoparticle form, are another excellent adsorbent choice due to their low toxicity and high thermal stability, surface area, and porous structure [29]. Generally, pure metal oxides exhibit reduced fouling and wetting in membrane matrices due to their superhydrophobic or amphiphilic nature [30]. When incorporated into nanocomposites with precise structure, crystallinity, and surface properties, metal oxides serve as large bandgap energy semiconductors that are both non-toxic and water-stable. These semiconductor nanomaterials play a crucial role in photocatalytic processes, requiring the generation of oxygen. By absorbing photons, they increase oxygen vacancies, thereby facilitating the conversion of organic pollutants into low or intermediate hazardous byproducts such as carbon dioxide, water, and inorganic ions [31]. Carbon nanomaterials were altered with metal oxides, including aluminum oxide (Al_2O_3,) in recent work. The study indicated that the nanomaterials greatly increased 2-NP and Cr^{3+} adsorption [32]. This discovery suggests that combining carbon nanomaterials with metal oxides can improve water treatment systems for varied contaminants.

The recent use of Response Surface Methodology (RSM) to frame experimental research, particularly in water treatment, is noteworthy [33]-[36]. This method is increasingly used to assess and alter water filtration system operational parameters. RSM has helped researchers construct trials that quickly evaluate the complex interactions between treatment parameters, improving pollution removal and water quality. This unique application shows RSM's crucial role in water treatment development through rigorous experimental design and optimization.

This study aims to enhance the removal efficiency of 2-NP and Cr^{3+} through adsorption using (CNAs/Al_2O_3) by integrating RSM to fine-tune the adsorption performance. CNAs, composed of carbon nanotubes and carbon nanofibers were utilized for this purpose. The significance of this research lies in its potential to effectively remove the contaminants from water with the aid of RSM.Al_2O_3 serving as an adsorbent, offers a promisingly efficient and cost-effective method for water purification. Its properties enable it to attract and bind specific contaminants, thereby facilitating their removal from water. Therefore, insights gained from this research could lead to scalable water treatment solutions that can be implemented in various settings, from small-scale local systems to large-scale industrial applications.

2. Materials and method

2.1 Materials and Chemicals

In this study, we used Conical Carbon Nanofibers (CCNFs) supplied by Hebei Liche Zhuoge Environmental Technology Co., Ltd, selected for their exceptional purity of 99.99%. Their effectiveness has been demonstrated in previous studies [35], [36] and further documented in additional academic articles [37], [38], [39]. These CCNFs featured diameters ranging from 75 to 25 nm and lengths between 20 to 30 m. The study also used MWCNTs (Multi-Walled Carbon Nanotubes) sourced from Sigma Aldrich, characterized by a minimal trace metal presence below 2000ppm, with average and outer diameters of 8.7 nm and 6.0 nm respectively, lengths from 2.5 to 20μm, an inner diameter of 2.0 nm, and a purity of 98.99%. All reagents utilized were of analytical quality, including $(Al(NO_3)_3 \cdot 9H_2O)$ at 98% purity, 2-Nitrophenol ($C_6H_5NO_3$) in powder form, $Cr(NO_3)_3$ at 98.5% purity, along with (NaOH), (HNO_3) , (C_3H_6O), and C_2H_5OH, all meeting high purity standards of at least 98%.

2.2 Synthesis of (CNAs/ Al_2O_3)

Our earlier research capped Al_2O_3 deposition on carbon nanostructures (CNAs) at 20% to preserve their adsorptive properties, which can decline with too much metal oxide. Metal impregnation ratio, sonication time, and calcination temperature were found to improve the CNA/Al_2O_3 composite's 2-NP and Cr^{3+} adsorption. The synthesis was conducted following the procedures documented by Kabbashi, Ihsanullah, Zhao, and Al-Khaldi et al. [36], [40], [41], [42], respectively. Initially, carbon nanotubes (CNTs) and carbon nanofibers (CNFs) underwent an acid purification process using 1.0MHCl(35%). This was followed by filtration and thorough rinsing until reaching a neutral pH, which indicated the removal of acid and other impurities. The materials were then dried overnight at 80°C. This acid wash process significantly improved the adsorptive surface area of both the CNTs and CNFs. While the synthesis of nanocomposites through the integration of carbon nanostructures and metal oxides has been described by Asmaly H., Gouda, Natrayan, and Atieh, as cited in references [32], [37], [38], [39]. The synthesis of CNAs /Al_2O_3 started by mixing 100mg each of CNTs and CNFs in 50ml centrifuge tubes, ensuring an even distribution of the carbon nano adsorbents using a vortex mixer. In the subsequent stage of impregnation, different amounts of Aluminium Nitrate as specified in Table 1. (Figure 1) were each dissolved in 20ml of deionized water, stirring slowly for an hour. Following this, 200mg of CNAs were incorporated into each Al_2O_3 solution across three 100ml beakers, stirred smoothly for two hours. Each beaker's contents, comprising CNAs and Al, were then mixed with 50ml of 99% ethanol, stirring for half an hour. Afterward, the mixture was allocated into small pots, marked as outlined in Figure 1, according to the experimental Design layout. The sonication time and drying steps were adjusted as per the experimental Design layout. The sonication time and drying steps were adjusted as per the experimental software's advice to remove any residual moisture and ethanol. The calcination process was carried out at specific temperatures to get rid of organic and nitrate debris, thereby enabling the Al_2O_3 particles to bind to the surfaces

of the CNAs. The concluding phase involved cleansing and desiccating the samples at 80°C for a day, preparing them for their role in adsorbing 2-NP and Cr^{3+}.

Figure 1: *The Prepared samples of CNAs with three ratios of* Al_2O_3 *at different conditions.*

Table 1: *The factors and their levels for adsorption of 2-NPh and* Cr^{3+}

Factor	Name	Units	Min	Max	Coded Low	Coded High	Mean	Std. Dev.
A	Al impregnation-Ratio	%	18.00	22.00	-1 ↔ 18.00	+1 ↔ 22.00	20.00	1.630
B	Sonication Time	hr	1.0000	3.00	-1 ↔ 1.00	+1 ↔ 3.00	2.00	0.8165
C	Calcination Temperature	C	300.00	500.00	-1 ↔ 300.00	+1 ↔ 500.00	400.0	81.65

2.3 The stock solution and adsorption studies

A 2-NPh solution of 1000ppm was prepared by dissolving 1.0gram of 2-NPh powder in 1000 mL of deionized water, and a similar concentration solution for Cr^{3+} was made using 4.578 grams of Chromium Nitrate anhydrate in water. Both were diluted to create a 50 – ppm stock solution, with magnetic stirring ensuring uniform dispersion. pH adjustments were made using nitric acid (HNO_3) and sodium hydroxide (NaOH), supported by buffer solutions for stability. The adsorption efficacy of CNAs /Al_2O_3 composites at ratios of 18%, 20%, and 22% was tested for 2-NPh and Cr (III) removal under controlled conditions at 25.0°C, using an orbital shaker for consistent agitation. The setup involved a 10-hour contact time, 300rpm agitation, pH6.50, 20mg of adsorbent, and an initial concentration of 50mg/L. Final concentrations were measured in 100ml flasks, ensuring accuracy by cleaning all glassware with a 5% nitric acid solution and 99.9% Acetone to avoid metal ion contamination. The equilibrium concentration of 2-NP was determined at a maximum absorbance of 317.5 nm using a UV-VIS Spectrophotometer (Jasco V-750), while Cr^{3+} levels were measured with an Atomic Spectrometer Analyzer (Perkin Elmer ASA 700). This method facilitated the calculation of adsorption capacities for both 2-NPh and Cr^{3+} using equation (1), highlighting the composites' effectiveness in pollutant removal from aqueous solutions.

$$Qe = \left(\frac{C_i - C_e}{M_{\text{adsorbent}}} \right) * V_{\text{sol}} \tag{1}$$

Q represents the adsorption capacity (mg/g), where C_i is the initial concentration of the adsorbate in the liquid phase (mg/L), and Ce refers to the equilibrium concentrations of the adsorbates 2-NPh

and Cr^{3+} in the solution (mg/L). V_{sol} denotes the total volume of the adsorbate solution used (L), and Adsorbent is the mass of the CNAs/ (Al_2O_3) adsorbent (g).

2.4 Characterization Techniques

To evaluate the effects of varying aluminium concentrations impregnated onto Carbon Nano Adsorbents (CNAs) utilized energy dispersive X-ray spectroscopy (EDX) for elemental analysis. EDX played a critical role in verifying the presence and measuring the precise weight of aluminium deposited onto the CNAs. This analytical method was integral in quantifying the aluminium content within the fabricated CNAs. To assess the adsorption characteristics and surface areas of the CNAs under different synthesis conditions, including variable calcination temperatures, nitrogen adsorption/desorption isotherms were recorded at 77.35 K using the Micromeritics ASAP2020 system. Prior to these measurements, the samples were subjected to degassing. The Brunauer-Emmett-Teller (BET) method was then applied to calculate the specific surface areas, which is essential in understanding the influence of different aluminium loadings and synthesis parameters on the adsorption properties of the CNAs.

2.5 Analysis of Response Surface Method (RSM)

Response Surface Methodology (RSM) employs mathematical and statistical techniques to design experiments, build models, examine operational variables, and identify the optimal conditions for achieving a specific outcome [44,45]. In our research, we conducted experiments across the range of each factor to determine the best conditions for adsorbing 2-NP and C^{3+} from water using RSM. By pinpointing the impregnation ratio, calcination temperature, and sonication duration as key factors in the adsorption process, we refined our models through RSM. Our study implemented the Central Composite Design (CCD) component of Response Surface Methodology (RSM) to determine the most efficient settings for the removal of Cr (III) and 2-NP. Table 2 presents the coded factors and their associated values for the adsorption experiments conducted through RSM. We employed Analysis of Variance (ANOVA) for data assessment, utilizing Design Expert Version 13 software (Stat-Ease, USA). The experimental setup featured 16 runs, encompassing 16 factorial points (including two repeats), 2 central points, and 1 axial point (with a single repetition). Additionally, we adjusted the (alpha at 1.0) aiming for a 95% confidence level in our findings.

3. Result and discussion

3.1 Adsorbents Characterization

3.1.1 Dispersive X-ray Spectroscopy (EDX)

EDX was employed to explore how the aluminum oxide integrates into Carbon Nano Adsorbents (CNAs) at concentrations of 18%, 20%, and 22% Al. This technique allowed for the precise quantification of Al within the CNAs by assessing changes in the elemental composition, particularly the oxygen and aluminum percentages. The EDX analysis revealed distinct Al peaks, confirming the accurate measurement of Al nanoparticle content in the CNAs. A notable reduction in carbon content was observed, decreasing from 83.62% in CNAs with 18%Al to 67.76% in those with 22%Al, indicating successful Al integration. Concurrently, oxygen content increased from 10.152% to 12.41%, correlating directly with the Al concentration and reflecting Al 's oxygen component. The proportion of Al itself rose from 16.23% in the 18%Al samples to 19.83% in the 22%Al samples, underscoring the effective amalgamation of Al into the CNAs. Integrating Al at three specific ratios into the Carbon Adsorbent, as confirmed by Energy Dispersive X-ray (EDX) analysis, facilitated the development of an innovative composite consisting of CNAs and Al_2O_3. This highlights the success of the approach in engineering superior adsorbent composites (Figure 2).

Fig. 3(a–i) showcases EDX spectroscopy maps for Carbon Nano Adsorbents, highlighting the variations in the spatial distribution of Aluminium (Al), Carbon, and Oxygen with Al content ratios

Table 2: *ANOVA analysis of variance of the quadratic model for Adsorption 2-NPh & Cr^{+3}*

Response	Source	Sum of Squares	df	Mean Square	F-value	p-value		Fit Statistics
	Model	2512.21	8	314.03	140.65	<0.0001	significant	
	A-Impregnation Ratio	1444.94	1	1444.94	647.2	<0.0001		
	B-Sonication Time	24.86	1	24.86	11.13	0.0125		SD=1.49
	C-Calcination Temp	623.88	1	623.88	279.44	<0.0001		Mean = 61.98
	AB	41.85	1	41.85	18.75	0.0034		C.V%= 2.41
	AC	42.47	1	42.47	19.02	0.0033		R^2= 0.9938
	BC	162.32	1	162.32	72.71	<0.0001		AdjR^2= 0.9868
Adsorption Capacity (mg/g)	A^2	165.07	1	165.07	73.94	<0.0001		Pred R^2= 0.947
of 2-NPh	B^2	13.61	1	13.61	6.1	0.0429		AP= 39.5067
	Residual	15.63	7	2.23				
	Lack of Fit	15.6	6	2.6	93.06	0.0792		
	Pure Error	0.0279	1	0.0279			not significant	
	Cor Total	2527.83	15					
	Model	986.69	9	109.63	122.35	<0.0001	significant	
	A-Impregnation-Ratio	43.78	1	43.78	48.85	0.0004		
	B-Sonication Time	442.54	1	442.54	493.87	<0.0001		SD= 0.9466
	C-Calcination Temp	9.33	1	9.33	10.41	0.018		Mean = 83.19
	AC	6.08	1	6.08	6.79	0.0404		C.V%=1.14
	BC	8.09	1	8.09	9.03	0.0238		R^2=0.9946
Adsorption Capacity (mg/g)	A^2	19.03	1	19.03	21.24	0.0037		Adj R^2= 0.9865
of Cr+3	B^2	309.29	1	309.29	345.17	<0.0001		Pred R^2= 0.9605
	C^2	155.39	1	155.39	173.41	<0.0001		AP=43.1232
	Residual	33.96	1	33.96	37.89	0.0008		
	Lack of Fit	5.38	6	0.8961			not significant	
	Pure Error	4.8	5	0.9602	1.67	0.5262		
	Cor Total	0.5756	1	0.5756				

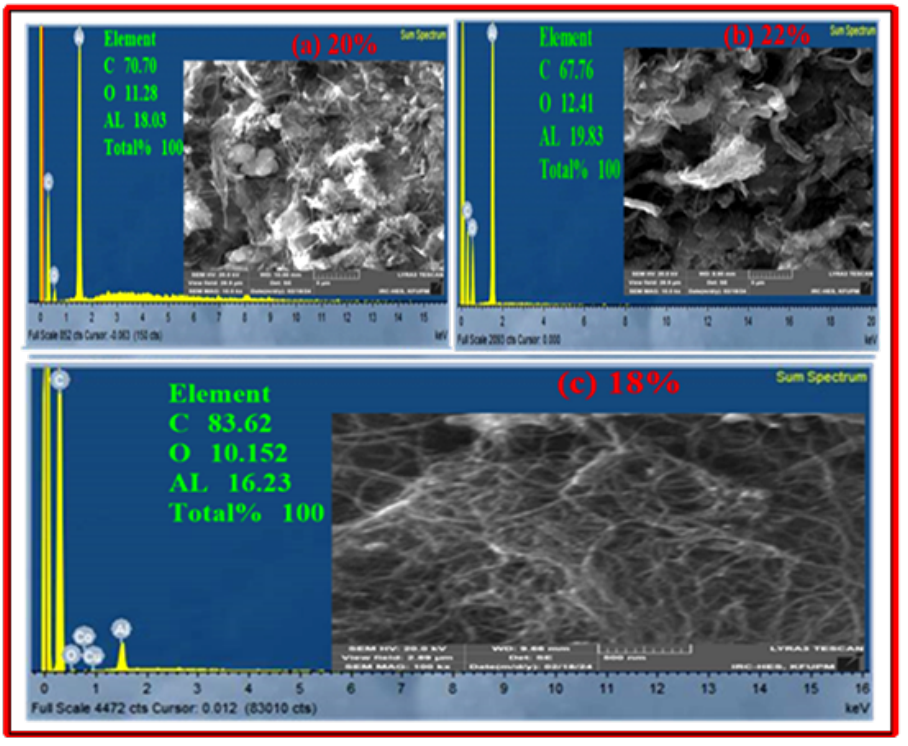

Figure 2: *EDX Spectrums of the CNAs with different ratios of AL.*

of 20,22, and 18. The Aluminium maps indicate a progression in saturation: a deep purple at 20% (Figure 3d) signifies uniform distribution, which intensifies to a denser purple at 22% (Figure 3a) and lightens at 18 percent (Figure 3g), indicating varying Aluminium concentrations. Carbon displays a transition from moderate white specks at 20% (Figure 3e), representing a dispersed distribution, to a denser speckle at 22% (Figure 3b), and then to a sparser pattern at an 18% (Figure 3h), suggesting changes in Carbon density. Similarly, Oxygen's speckling pattern starts sparse at a 20% (Figure 3f), becomes denser at 22% (Figure 3c), and then sparser again at 18% (Figure 31). The EDX maps collectively illustrate that an increase in the AI ratio correlates with a more pronounced and uniform elemental concentration and distribution. The maps at a 20%Al provide a baseline for understanding the elemental spread, those at a 22 % suggest an enhanced and possibly more uniform elemental presence, and the maps at an 18% Al depict a lighter and more varied elemental distribution within the adsorbents.

3.1.2 BET Surface Area Analysis

The study analysed the surface areas of three CNAs/Al_2O_3 composites with aluminium oxide contents of 18%, 20%, and 22%, following 3 hours of sonication and calcination at 300°C, 400°C, and 500°C, respectively. Using the nitrogen adsorption/desorption isotherm method at 77 K, specific surface areas were calculated based on BET equations. This analysis is crucial for evaluating how aluminium oxide impregnation affects CNAs' surface area and their effectiveness in removing pollutants like 2-NPh and Cr^{3+} from water. It explores the impact of varying aluminium oxide proportions on the adsorption/desorption properties of CNAs, suggesting that metal oxide incorporation can enhance the adsorbent's surface area by increasing adsorption sites (Figure 4). Aluminium oxide's

presence significantly enhances CNAs' external surface without altering their internal structure, thus increasing their effective surface area. Comparing three CNAs/Al_2O_3 samples prepared with different aluminium oxide ratios and calcination temperatures showed a decrease in surface area with higher aluminium content and calcination temperature. Specifically, the 18%, 20%, and 22%Al-loaded CNAs showed surface areas of 176 m^2/g, 125 m^2/g, and 110 m^2/g, respectively. This trend indicates that higher Al oxide levels might block CNAs' pores, diminishing their adsorption capacity. Furthermore, samples calcined at 500°C had lower surface areas than those at 300°C, suggesting that lower temperatures maintain CNAs' porous structure, boosting adsorption efficiency. The significant difference in surface area among the CNAs/Al_2O_3 variants, especially the larger surface area of 176 m^2/g for the 18%Al sample compared to the 110 m^2/g and 125 m^2/g for the 22% and 20% samples, highlights aluminium oxide content's critical role in determining the adsorptive qualities of these nanomaterials.

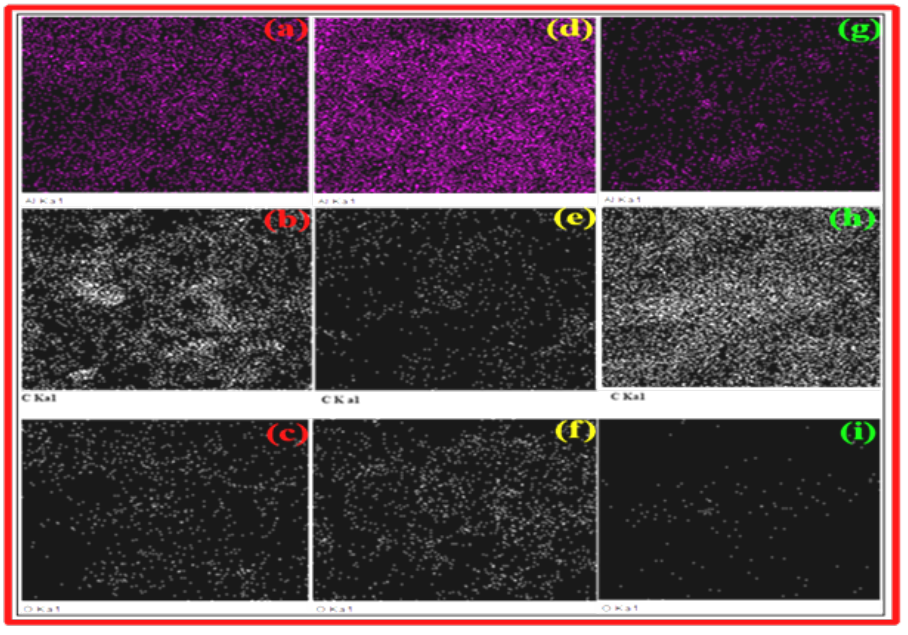

Figure 3: *EDX elemental mapping of Synthesised CNAs with* 20%Al (a_1, b_2c), 22%Al (d_1, e_2) *and 18 % Al(g, h, i)*

3.2 Analysis of Adsorption Study

The analysis of 2-NPh using UV spectrometry, as depicted in Figure 5a, revealed its peak absorbance at a wavelength of 317.5 nm with a recorded absorbance value of 1.27125 , at a starting concentration of 50ppm. The equilibrium concentrations post-shaking for each experimental run were determined from their respective absorbance values. Figure 5b indicates that these equilibrium concentrations differed across experimental runs, which is attributed to the alterations in the conditions under which the Carbon Nano Adsorbents (CNAs) were prepared, impacting the absorption process. The resulted adsorption capacities derived from equation (1) detailed in Table 3. This data demonstrates how experimental variables influence adsorption effectiveness. Further output in Figure 6a revealed the maximum adsorption capacity at 82.019mg/g during run 12 , with conditions of an 18% Aluminum ratio, 300°C calcination, and 3 hours of sonication. In contrast, the minimum capacity of 37.6mg/g was noted in run 14, under conditions of a 22% Aluminum ratio, 500°C calcination, and 1 -hour

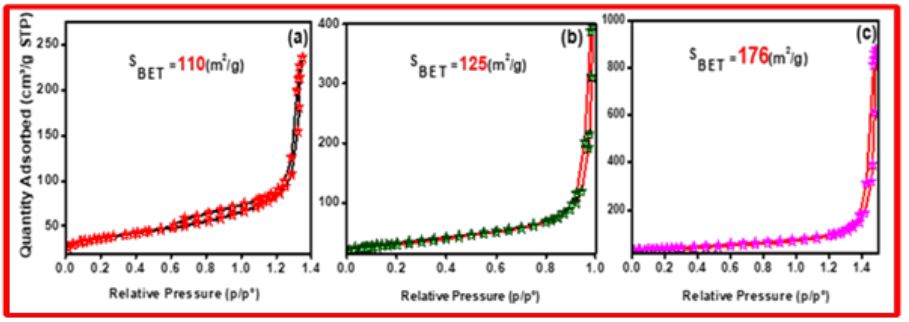

Figure 4: *Surface area measurements of CNAs loaded by Aluminum at conditions (a)* 22%Al *(3hrs,* 500C *) (b)* 20%Al *(3hrs, 400C) (c)* 18%Al *(3hrs and 300C).*

sonication. This variation of the results highlights the significant impact of procedural parameters on adsorption efficiency. This thorough analysis not only identifies the optimal adsorption conditions for 2 – NPh but also underlines the importance of systematic experimental planning in improving adsorption performance. An in-depth review of the adsorption capacities for all runs, considering their interactions and the optimization via Response Surface Methodology (RSM) discussed in section 3.4.

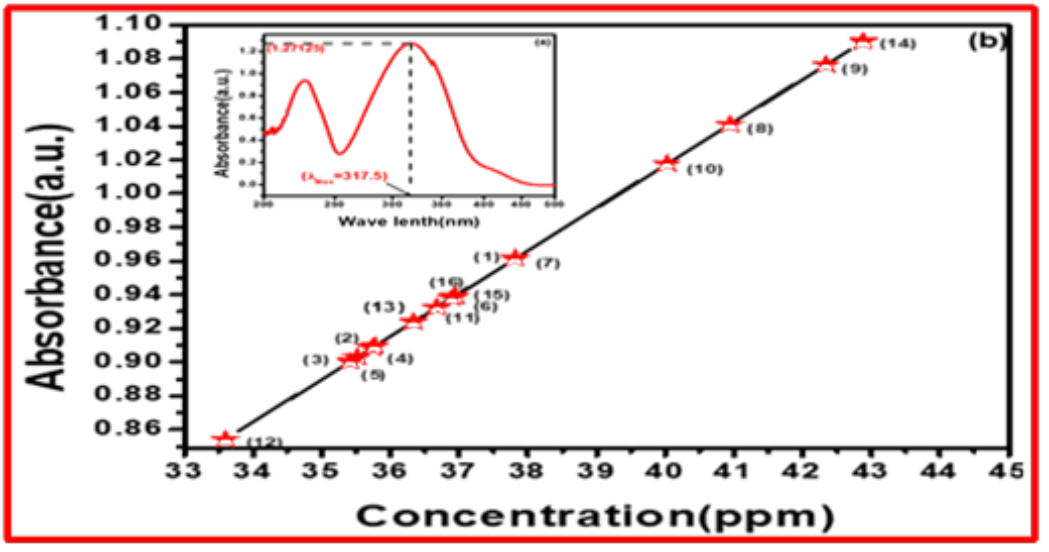

Figure 5: *Adsorption process of the* 2 – NPh *(a)Absorbance spectra at Init-Con-at* (λ max = 317.5) *(b) Corresponding Concentration for each experimental run Label.*

Alternatively, the Atomic Spectrometer Analyzer was employed to determine the equilibrium concentration of Cr^{3+}, revealing an absorbance of 0.466 at an initial concentration of 50ppm. Subsequent calculations of adsorption capacity for each sample, as delineated by equation (1). The apex of adsorption efficiency was observed in sample 12, boasting an adsorption capacity of 96.6mg/g (Figure 6b), achieved through a configuration of 18% aluminum loading, 3 hours of sonication, and a calcination temperature of 300°C. Conversely, the nadir of adsorption efficiency was noted in sample 13 , with a capacity of 64.4mg/g, attributed to a 22% aluminum loading, one hour of

sonication, and a calcination temperature of 400°C.

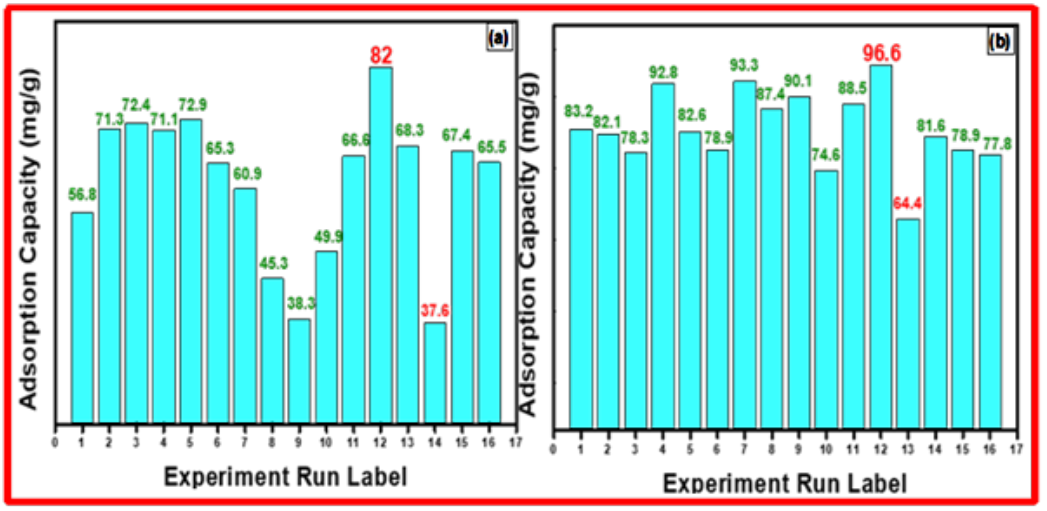

Figure 6: *Obtained Absorption Capacity of* CNA/Al_2O_3 *values Influenced by different Parameters for the Adsorption of (a)* 2 – NPh *(a) (b)* Cr^{+3}.

The sonication time, aluminium loading mass, and calcination temperature will explain the $CNAs/Al_2O_3$ adsorbent's Cr^{3+} and 2-NPh adsorption capacities. Figure 6 (a.b) shows that an 18% aluminium ratio, 3 hours of sonication, and 300°C calcination (Run Label 12) yielded the highest Cr^{3+} and 2-NPh adsorption capacities of 96.6mg/g and 82.0mg/g, respectively. With 22% aluminium loading, one hour of sonication, and 400/500°C calcination temperatures, both adsorbates had the lowest capacities, 64.4mg/g for Cr^{3+} (Run Label 13) and 37.6mg/g for 2-NPh (Run Label 14). Aluminium loading affects adsorption capacity, with a 22% loading reducing Cr^{3+} and 2-NPh adsorption efficiency, may be due to pore blockage, active site coverage, and competitive adsorption, compared to an 18% loading. This shows the critical balance needed to optimize adsorption capacity without compromising CNA structural and chemical integrity. These findings emphasize the importance of fine-tuning aluminium loading to achieve maximal performance by balancing its benefits and potential drawbacks. From 1 to 3 hours, sonication length significantly changes Carbon Nano Adsorbents (CNAs) structure. This effect depends on several factors. Sonication increases aluminium particle dispersion on CNAs, increasing adsorption surface area. Surface area directly affects adsorption capacity, offering more places for adsorbate molecules to adhere. Sonication time can also change CNA pore structure, possibly increasing pore size. Structural modifications allow bigger molecules or ions to adsorb into CNAs' internal adsorption sites. Extended sonication also evenly distributes aluminium oxide nanoparticles on CNAs, resulting in surface-wide adsorption. Because it permits the entire CNA surface to eliminate Cr^{+3} and 2-NPh evenly, homogeneity is essential for uniform and successful adsorption. Aluminium-doped (CNAs) adsorption effectiveness for Cr^{+3} and 2-NPh decreases when calcined at 500°C instead of 300°C due to high-temperature changes. Also, CNAs may lose surface area, porosity, and active adsorption sites at high temperatures, compromising their structural integrity. Additionally, the CNA surface chemistry changes, such as the reduction or alteration of essential functional groups like hydroxyl and carboxyl, which are needed for complexation or hydrogen bonding with adsorbates, worsen this deterioration. CNAs' pore structure deteriorates at 500°C calcination, inhibiting adsorbate transport into and within nanotubes. Aluminium particle may agglomeration on CNAs at higher temperatures promotes

uneven distribution and larger particle sizes, blocking pores and limiting sorption surface area. The absence of oxygencontaining groups makes CNAs more hydrophobic, which diminishes their affinity for polar molecules like 2-NPh, making the phase of aluminium oxide produced at these temperatures less effective at adsorbing Cr^{+3} and 2-NPh. These findings demonstrate the importance of calcination temperature on aluminium-doped CNA adsorptive properties.

Table 3: *The predicted and experimental adsorption capacity of 2-NPh and* Cr^{+3}

	2-NPh		Cr3+	
Run Order	Actual Value	Predicted Value	Actual Value	Predicted Value
1	56.78	57.42	83.15	83.53
2	71.32	71.61	82.08	81.79
3	72.42	73.79	78.33	78.78
4	71.13	69.84	92.81	91.90
5	72.93	73.22	82.62	81.60
6	65.29	65.32	78.86	78.97
7	60.92	61.18	93.35	93.75
8	45.27	45.80	87.45	87.71
9	38.29	37.11	90.13	89.83
10	49.86	49.79	74.57	74.33
11	66.63	66.52	88.52	88.98
12	82.02	81.38	96.57	96.92
13	68.32	65.90	64.38	64.64
14	37.56	38.39	81.55	81.36
15	67.40	69.05	78.86	77.95
16	65.52	65.32	77.79	78.97

3.3 Response Surface Method (RSM) results

Considering the purpose of this investigation, the Central Composite Design (CCD) was utilized to carry out a total of sixteen different experiments. The structure of the design and the adsorption capacities for 2 – NPh and Cr^{+3} is demonstrated in this experimental setup. A two-level, four-factor methodology, which is designated by the letter "k," was utilized in the experimental strategy. The total number of experiments could be computed by the formula 2 raised to the power of k. This methodical approach outlined the conditions for each of the sixteen experiments, which evaluated the effectiveness of (CNAs) modified with different ratios of Al_2O_3 in the removal of 2-NPh and Cr^{3+} from water. In the case of 2-NPh, the observed adsorption capacity ranged from 37.5607 to 82.021mg/g, but in the case of Cr^{3+}, the capacity ranged from 64.3777 to 96.5665mg/g. This demonstrates the variable efficacy of the adsorbents under different experimental settings.

3.4 ANOVA Analysis

ANOVA analysis was used to confirm the efficacy of the models proposed. research describes the results of fitting a second-order response surface model, specifically for 2- NPh and Cr^{3+} removal, as well as the yield of adsorption capacity. These models were evaluated according to their coefficient of determination (R^2) and standard deviation. Table 2 demonstrates that the models were statistically significant at the 95% confidence level, as shown by P-values less than 0.05 . An R^2 value approaching one and a reduced standard deviation suggest that a model has improved predictive accuracy. The

computed coefficients of determination for 2-NPh and Cr^{3+} adsorption capability (R^2 values of 0.9938 and 0.9946 , respectively) above the 0.80 criterion, suggesting a strong model fit. High R^2 values near unity indicate a significant agreement between predicted and actual outcomes within the experimental scope, emphasizing the necessity of matching the adjusted R^2 for correct model representation. The statistical analysis revealed that these models accurately predicted the outcomes for adsorption capacities for 2-NPh and Cr^{3+} within the parameters tested. Furthermore, the Adequacy Precision (AP) ratios, calculated at 39.5067 for 2 – NPh and 43.1232 for Cr^{3+}, were enough for model validation. AP ratios greater than 4 are desirable, demonstrating the models' capacity to effectively explore the design space defined by the Central Composite Design (CCD).

The coefficient of variance (CV), calculated as the standard error of estimate divided by the mean observed response value and given as a percentage, is a measure of the model's repeatability. A CV of 10% or below suggests that the model is replicable [30]. Th research shows that the CV values for the analysed responses are particularly low, at 2.41% for 2 – NPh and 1.14% for Cr^{+3}, with neither exceeding 3.00%. This investigation discovered that the quadratic models associated to these answers were significant, whereas words that did not contribute significantly to the models were removed to improve model performance. The results indicate that the response surface models developed for estimating the yield of 2NPh and Cr^{3+} removal, as well as adsorption capacity, were indeed reasonable. Equ (2 & 3) show precise second-order polynomial equations for the regression models, which reflect their coded factors, demonstrating their statistical value and predictive power in our investigation.

Adsorption Capacity

$$(2NPh) = 65.32 - 12.2\ A + 1.85\ B - 7.90C + 2.29AB - 2.30AC - 4.5BC - 7.5\ A^2 + 2.15\ B^2 \quad (2)$$

Adsorption Capacity

$$\left(Cr^{3+}\right) = 79.79 - 2.09\ A + 6.65\ B + 0.9657C - 0.8718AB + 1.01AC - 1.54BC + 10.83\ A^2 - 7.68\ B^2 + 3.56C^2 \quad (3)$$

Plots comparing predicted values to actual results are critical for determining a model's accuracy. The output predicted against actual values for 2 – NPh and Cr^{3+} adsorption, as well as their corresponding adsorption capacity yields, show an acceptable alignment between empirical data and model predictions (Table 3). This agreement indicates that the prediction models are reliable instruments for exploring the design space defined by the (CCD).

The DX13(Design Expert version 13) software was used to construct 3D surface response and contour plots to investigate the interactions between independent factors and their impact on model responses. The ANOVA results for the adsorption capacity of 2 – NPh revealed that the impregnation ratio (A) had the greatest impact, with an F-value of 647.20, followed by the calcination temperature (C), with an F-value of 279.44, and the sonication time (B), with an Fvalue of 11.33. In contrast, the sonication time (B) had the greatest influence on Cr^{3+} adsorption capacity, with an F-value of 493.87 , followed by the impregnation ratio (A), with an F-value of 48.85, and the calcination temperature (C), with an F-value of 10.41. This analysis reveals that the impregnation ratio and calcination temperature are more crucial for boosting 2-NPh adsorption by the CNAs/Al_2O_3, whereas sonication time and impregnation ratio significantly affect Cr^{3+} adsorption, more so than the calcination temperature.

3.5 The effect of Parameters on the Adsorption capacity

In Fi nalytical approach is utilized whereby one variable is maintained at a constant value to facilitate the manipulation of the remaining two variables within their experimental boundaries, enabling the examination of the interplay between impregnation ratio, sonication time, and calcination temperature on the adsorption of (2 – NPh), as depicted through threedimensional response surfaces.

Similarly, Figure 8 delves into the effects of these identical variables on the adsorption efficiency of Chromium, with experiments conducted at an optimal impregnation ratio of 18%, culminating in peak adsorption capacities of 82.01 for 2-NPh and 96.6 for Cr^{3+} at a 3-hour sonication and 300°C calcination. In contrast, minimal capacities of 37.6 for 2 – NPh and 64.4 for Cr^{+3} were observed at a 1-hour sonication and higher calcination temperatures of 400°C and 500°C, respectively. The contour plots generated illustrate a correlation between enhanced adsorption for both substances with increased sonication time and reduced impregnation ratio and calcination temperature, underscoring the importance of optimizing operational parameters. This comprehensive analysis suggests that carefully adjusting sonication duration and controlling calcination temperature can significantly enhance the removal efficiency of hazardous substances like 2NPh and Cr^{3+} from aqueous solutions, highlighting the nuanced interdependencies between variables and providing a roadmap for future environmental remediation studies.

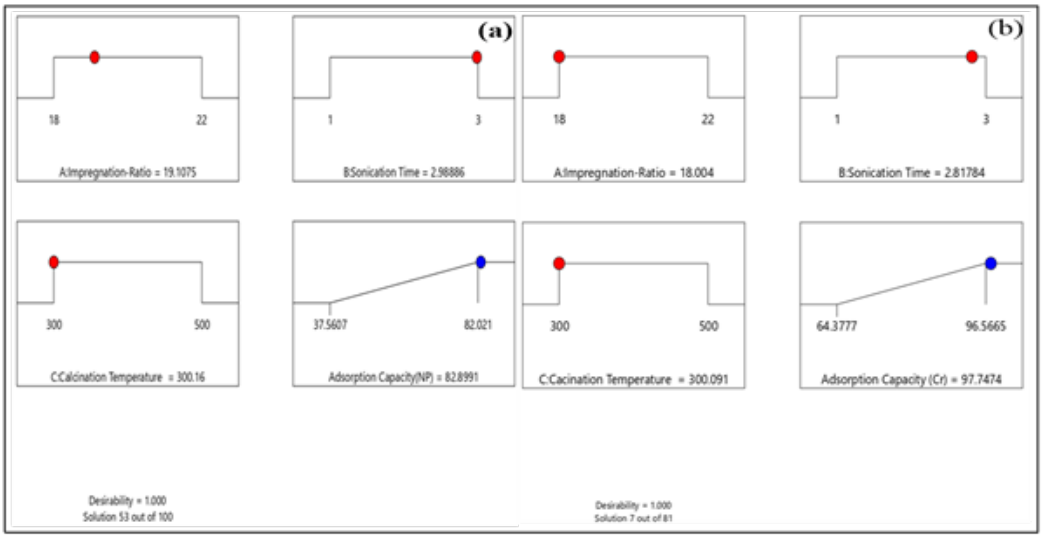

Figure 7: *The Optimized results for parameters and adsorption capacity for (a) 2-NPh(b) Cr^{3+}*

3.6 Optimization the Adsorption of 2-NPh and Cr^{3+}

Utilizing Design Expert 13 software, the optimization procedure was implemented to identify the ideal adsorption capacities for 2 – NPh and Cr^{3+} using CNAs in aqueous solutions under a variety of conditions. The optimization criteria as seen in Table 4 within the software were set to keep each operational parameter (Impregnation Ratio, sonication time, calcination temperature) 'within range', aiming for the maximal adsorption capacities for both 2-NPh and Cr^{3+} to ensure peak efficiency. The outcomes of the optimization for 2-NPh and Cr^{3+} are thoroughly presented in Tables 5 and 6. The high desirability score of 1.000 indicates excellent correlation between the predicted function and the experimental model under optimal conditions (Table 4). The optimal adsorption capacity for 2 – NPh was realized by employing a 19.1075% impregnation ratio, 2.9889 hours of sonication, and a calcination temperature of 300.160°C, which yielded an adsorption capacity of 82.8991mg/g, as depicted in Figure 7 and as plot of three dimension in Figure 8. Subsequent analysis of these optimization parameters through the predicted point in the Design of expert (DOE) led to a slightly improved adsorption capacity of 83.154mg/g as seen in confirmation step.

Absorbent hand, the most effective adsorption of Cr^{3+} was observed using a carbon nano adsorbent

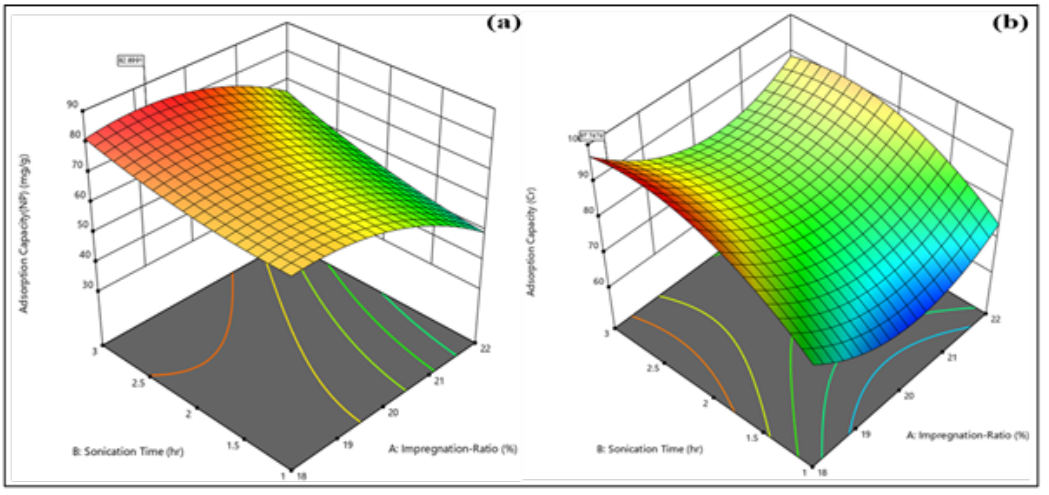

Figure 8: *Three-dimensional response surface for Optimized adsorption capacity at optimum conditions of (a)2-* NPh *(b)* Cr^{3+}.

Table 4: *Analysis Prediction Point and Confirmation with a 95% Confidence Level and 99% Population Accuracy*

Analysis	Predicted Mean	Predicted Median	Std Dev	SE Mean	95% CI low for Mean	95% CI high for Mean	95% TI low for 99% Pop	95% TI high for 99% Pop
Adsorption Capacity (2-NP)	83.154	83.154	1.49419	1.16024	80.4105	85.8976	74.039	92.269
Adsorption Capacity (Cr)	97.7981	97.7981	0.94660	0.773161	95.9063	99.69	91.6253	103.971

with an 18.00% loading, subjected to 2.81784 hours of sonication time, and calcined at a temperature of 300.091°C, achieving an adsorption capacity of 97.7474mg/g as shown in Figure 9 and as plot of three dimension in Figure 10. Further post-optimization analysis through the Predicted point step in the (DOE) revealed an even slightly higher adsorption capacity of 97.7981mg/g as seen in confirmation step, obtained under slightly modified optimal conditions: an 18% impregnation ratio, 2.41 hours of sonication, and a calcination temperature of 301°C.

3.7 Validation of the Adsorption capacity values

The synthesis of Carbon Nano Adsorbents (CNAs) for maximal adsorption capacity followed the optimal conditions identified through optimization, leading to the creation of CNAs with a composition of 19%Al, undergoing 3 hours of sonication period at a calcination temperature of 300°C, specifically targeting the adsorption of 2-Nitrophenol (2-NP). In contrast, the synthesis of CNAs/Al for Chromium (Cr^{3+}) adsorption incorporated a slightly different protocol: 18%Al, with 2.4 hours of sonication at a calcination temperature of 301°C. The prepared adsorbent under this condition were applied used through the adsorption process again and obtained adsorption capacity.

Table 5 meticulously contrasts the adsorption capacities of both 2-NP and Cr^{3+}, aligning initial,

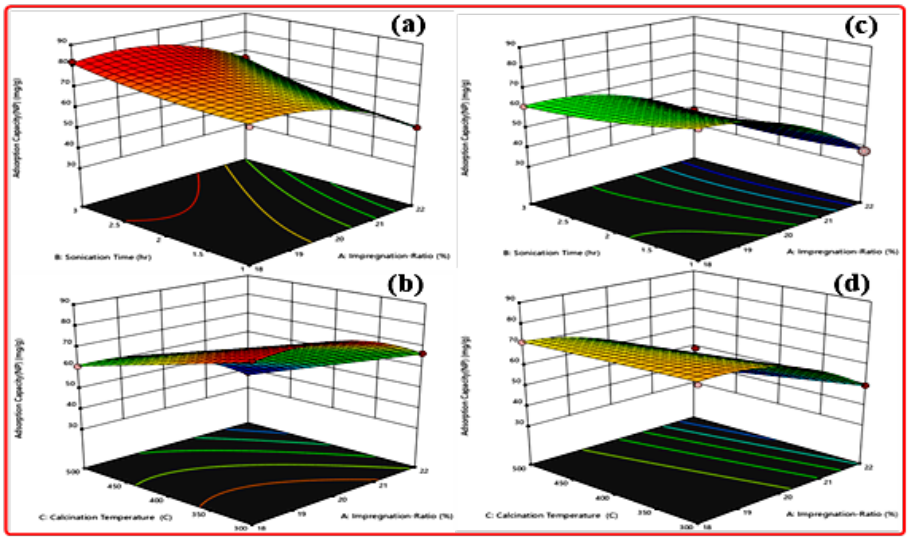

Figure 9: *The (3D) surface plot of interaction parameter of impregnation ratio with sonication time and Calcination Temperature at Max adsorption capacity (a,c) and Min adsorption capacity (b,d) of 2-NP.*

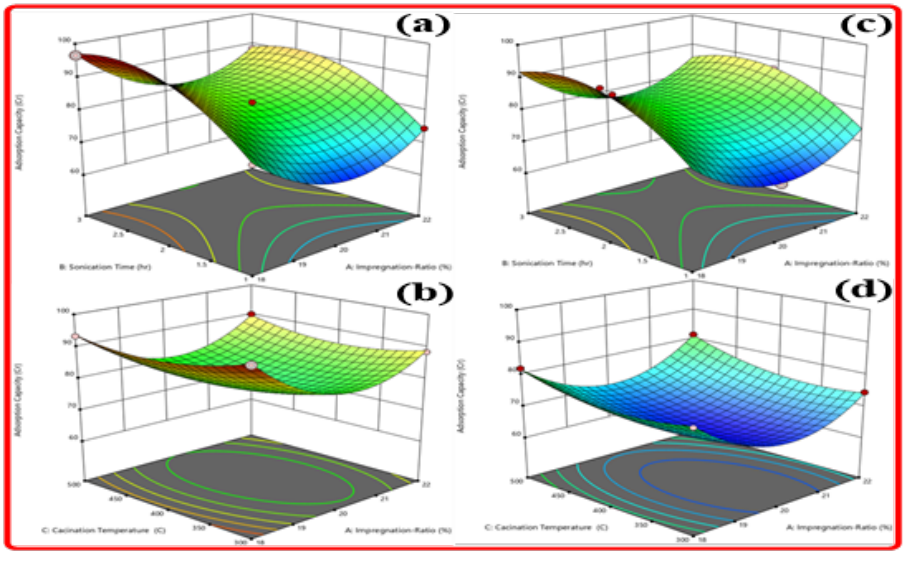

Figure 10: *The (3D) surface plot of interaction parameter of impregnation ratio with sonication time and Calcination temperature at Max adsorption capacity (a,c) and at Min adsorption capacity (b,d) of* Cr^{3+}

optimized, and validated experimental findings, and the percentage of Error can calculate from equation (4):

$$\text{Error\%} = \left(\frac{\text{optimized Value-Validated Value}}{\text{optimized value}} \right) * 100\% \quad (4)$$

The validation process for 2-NP adsorption registered a capacity of 86.793mg/g, showing a deviation of about ~ (5%) from the anticipated optimal value of 83.154mg/g. On the other hand,

Table 5: *Validating the Adsorption Capacity Measurements for This study.*

Adsorbate	Ratio of Al %	Sonication Time(hr)	Calcination Temp(C)	Abs (50ppm= 1.25125)	Abs (50ppm= 0.466)	Equilibrium Con(ppm)	Qe (mg/g
2-NP	19	3	300	0.82991	——	32.6415	86.7925
Cr3+	18	2.4	300	——	0.280	30.0429	99.7854

Cr^{3+} adsorption achieved a validated capacity of 99.785mg/g, diverging by ~ (2%) from its projected optimal of 97.80mg/g. With the error margins for both adsorption studies staying below 10%, there's a strong alignment between theoretical predictions and real-world experimental outcomes, reinforcing the model's accuracy in forecasting the removal efficiencies for 2-NP and Cr^{3+} under the given experimental conditions.

Table 6: *Evaluating Adsorption Capacity Values Under Optimal Conditions*

Response	Initial Experimental Value	Optimized (Predicted) Value	Validation Experimental Value	Error %
Adsorption Capacity (2-NPh)	82.02	83.154	86.793	4.5
Adsorption Capacity (Cr3+)	95.57	97.80	99.785	2.0

3.8 Maximum adsorption Capacities for 2-NP and Cr^{3+} by different Adsorbent

Table 7 provides a concise summary of previous studies on the adsorption efficiency of various materials for (2-NP) and (Cr^{3+}). The adsorbents evaluated for 2-NP include alumina (Al_2O_3), HDTMA modified by Al_2O_3, iron oxide ($\alpha - Fe_2O_3$), carbon nano spheres, and several modified montmorillonite clays and zeolite minerals. Optimal adsorption capacities were typically observed at neutral pH levels, except for montmorillonite/BDHP, which required a strongly alkaline condition (pH10) to reach high adsorption capacity. Despite variations in the concentration of 2-NP and the amounts of adsorbents used across this different studies, all the experiments were consistently held at room temperature at 298 K. The adsorption capacity for 2-NP spanned from 6.05 to 86.8mg/g, with the CNAs/Al_2O_3 formulated in our current study demonstrating a remarkable capacity of 86.8mg/g. In the case of Cr^{3+}, effective adsorption capabilities were observed using granular activated carbon (GCA), natural mica, polyacrylamide-modified montmorillonite, zeolite processed from fly ash, and hydroxyapatite nanoparticles ranging from 7 to 99.8mg/g. Notably, the CNAs/Al_2O_3 produced in this research achieved an exceptional adsorption capacity of 99.8mg/g for Cr^{3+}, under conditions of pH6.0, a contaminant concentration of 50mg/L, and a 20mg adsorbent dosage, all at 298 K, indicating its superior adsorptive properties.

4. Limitations and Future Research Directions

Understanding the limitations of new adsorbent research is crucial for validating findings, enhancing efficiency, and ensuring real-world applicability. It also drives further research and is essential for assessing environmental and health impacts before widespread use, ensuring the safety and practicality of the adsorption process. The following points are suggested to address limitations and enhance the effectiveness and safety of the adsorption process of this study:

a. The study did not explore the possibility of increasing the ratios of CNTs and CNFs in the new composite, which could have improved the adsorption process due to variation on the surface

Table 7: *Compare the Absorption Capacity of 2- NP and Cr^{3+} with previous studies.*

Adsorbate	Adsorbent	Experimental condition				Adsorption Capacity	Reference
		pH	Concentration (mg. L-1)	Dosage mg	T K?	(mg/g)	
2-NPh	Al_2O_3	6	20	10	298	6.18	[46]
	HDTMA / Al_2O_3	6	20	10	298	9.05	
	α – Fe2O3	7	50	5	303	66.4	[47]
	Carbon Nano Spheres	7	20	20	298	32.9	[48]
	Montmorillonite /BDP	10	100	80	298	76.9	
	Montmorillonite /BDHP	10	100	80	298	81.3	[49]
	Zeolites	4	500	100	298	85.5	[50]
	CNAs / Al_2O_3	6	50	20	298	86.8	This study
Cr^{3+}	MWCNT	3	10	30	298	3.18	[51]
	GCA	7	10	40	293	7	[52]
	Muscovite mica	7.2	May-50	1	298	15.6	[53]
	Polyacrylamide-montmorillonite	5.5	0-300	1	298	59.7	[54]
	Zeolite A from fly ash	4	0-160	10	298	46.8	[55]
	Hydroxyapatite nanoparticle	10	Oct-70	4	298	96.9	[56]
	CNAs / Al_2O_3	6	50	20	298	99.8	This study

area as well as the porosity. It also did not investigate aluminum oxide proportions at low level such as 5% which could be important for future research. Further research is needed to determine the composite adsorbent's efficacy against a wider variety of contaminants, especially heavy metals.

b. The study did not investigate the optimum pH for the adsorption of pollutants and conducted the adsorption at neutral range specific (pH6.5).

c. The study did not address how variations in the composition of water sources in real-world applications might impact the effectiveness of the adsorbent under conditions that differ from those in controlled experiments.

d. The study did not address the long-term stability and reusability of this new absorbent, which are crucial for practical and economical water treatment solutions.

e. The study did not include the environmental impact of discarding or recycling the adsorbent, including pollutant leaching. Nano adsorbent in water is reactive and tiny, posing health risks to humans and wildlife. The study did not examine how nano adsorbents could accumulate in aquatic and terrestrial species, altering ecosystems, or how inappropriate disposal can harm the environment, underlining the necessity for adequate disposal procedures.

Here are several potential directions for future research opportunities:

i. Investigate different ratios of Carbon nanomaterials and metal oxides to extend the range of pollutants that can be removed from water.

ii. Conduct tests in various real-world settings to assess how different water compositions impact adsorbent performance.

iii. Focus on refining manufacturing and application processes to facilitate smoother transitions from laboratory to industrial scales.

iv. Examine the regeneration and repeated use of adsorbents to determine their economic efficiency and sustainability.

v. Perform detailed lifecycle and environmental impact studies on adsorbents, including their disposal and recycling methods, to ensure their safe and sustainable use.

By overcoming these limits and exploring these future research directions, the field can develop more long-lasting, efficient, and environmentally friendly adsorption technologies for water purification.

5. Conclusion

In this study, a Central Composite Design (CCD) was employed to enhance the adsorption effectiveness of CNAs/Al_2O_3 composites for the removal of 2 – NPh and Cr^{3+} from aqueous solutions. The results indicated that the impregnation ratio and calcination temperature had a greater impact on the adsorption of 2-NPh, whereas for Cr^{3+}, the impregnation ratio and sonication time were more influential than calcination temperature. EDX analysis confirmed the presence of aluminum oxide in the composites, and BET surface area measurements revealed a correlation between adsorption capacity and aluminum oxide content. The study achieved optimum adsorption capacities for CNAs, which surpassed many previous records, with 2 – NPh reaching 86.79mg/g under conditions of a 19% aluminum impregnation ratio, 3 hours of sonication, and a calcination temperature of 300°C. For^{3+}, the optimum capacity was 99.79mg/g, achieved with an 18% aluminum impregnation ratio, 2.5 hours of sonication, and the same calcination temperature.

Conflicts of Interest: **The authors declare no conflict of interest.**

NOMENCIATURE

CNAs Carbon Nano adsorbent
CCNFs Conical Carbon nanofibers
CSAC Char of South African coal
CNAs / Al_2O_3*CarbonNanaadsorbent/aluminiumoxide*

GAC Granular activated carbon
HDMB / Al_2O_3*hexadecyltrimethylammoniumbromide/AluminiumoxideComposite*
MWCNTs Multi wall carbon nanotubes
M/BDP Montmorillonites /(1,3-bis(dodecyldimethylammonio)-propane dibromide

References

[1] S. Mansoor et al., "Heavy metal induced oxidative stress mitigation and ROS scavenging in plants," Plants, vol. 12, no. 16, p. 3003, 2023.
[2] R.-Y. Li et al., "Heavy metal ions exchange driven protein phosphorylation cascade functions in genomic instability in spermatocytes and male infertility," Nucleic Acids Res., vol. 51, no. 7, pp. 3150–3165, 2023.
[3] W. Duan et al., "Levels of a mixture of heavy metals in blood and urine and all-cause, cardiovascular disease and cancer mortality: A population-based cohort study," Environ. Pollut., vol. 263, p. 114630, 2020.
[4] H. Rüdel, W. Körner, T. Letzel, M. Neumann, K. Nödler, and T. Reemtsma, "Persistent, mobile and toxic substances in the environment: a spotlight on current research and regulatory activities," Environ. Sci. Eur., vol. 32, no. 1, p. 5, 2020.
[5] S. E. Hale et al., "Getting in control of persistent, mobile and toxic (PMT) and very persistent and very mobile (vPvM) substances to protect water resources: strategies from diverse perspectives," Environ. Sci. Eur., vol. 34, no. 1, p. 22, 2022.
[6] T. Pavesi and J. C. Moreira, "Mechanisms and individuality in chromium toxicity in humans," J. Appl. Toxicol., vol. 40, no. 9, pp. 1183–1197, 2020.
[7] T. Xu et al., "Effect of soil pH on the transport, fractionation, and oxidation of chromium (III)," Ecotoxicol. Environ. Saf., vol. 195, p. 110459, 2020.
[8] L. Ju et al., "Formation, stability and mobility of soluble Cr (III) during Cr (VI) reduction by Pannonibacter phragmitetus BB," Environ. Technol. Innov., vol. 27, p. 102496, 2022.
[9] B. Jiang et al., "The reduction of Cr (VI) to Cr (III) mediated by environmentally relevant carboxylic acids: state-of-the-art and perspectives," J. Hazard. Mater., vol. 365, pp. 205–226, 2019.
[10] M. Tumolo et al., "Chromium pollution in European water, sources, health risk, and remediation strategies: An overview," Int. J. Environ. Res. Public Health, vol. 17, no. 15, p. 5438, 2020.
[11] H. Hashemi-Moghaddam and F. Abbasi, "Synthesis of molecularly imprinted polymers coated on silica nanoparticles for removal of p-nitrophenol from crude pharmaceuticals," Pharm. Chem. J., vol. 49, no. 4, pp. 280–286, 2015.
[12] P. Iwaniuk, S. Łuniewski, P. Kaczyński, and B. Łozowicka, "The influence of humic acids and nitrophenols on metabolic compounds and pesticide behavior in wheat under biotic stress," Agronomy, vol. 13, no. 5, p. 1378, 2023.
[13] A. Das and A. Dey, "P-Nitrophenol-Bioremediation using potent Pseudomonas strain from the textile dye industry effluent," J. Environ. Chem. Eng., vol. 8, no. 4, p. 103830, 2020.
[14] P. S. Pauletto, J. Moreno-Pérez, L. E. Hernández-Hernández, A. Bonilla-Petriciolet, G. L. Dotto, and N. P. G. Salau, "Novel biochar and hydrochar for the adsorption of 2-nitrophenol from aqueous solutions: An approach using the PVSDM model," Chemosphere, vol. 269, p. 128748, 2021.
[15] Z. Zhang, Y. Yu, H. Xi, and Y. Zhou, "Inhibitory effect of individual and mixtures of nitrophenols on anaerobic toxicity assay of anaerobic systems: Metabolism and evaluation modeling," J. Environ. Manage., vol. 304, p. 114237, 2022.
[13] O. A. Alsager, A. A. Basfar, and M. Muneer, "Decomposition byproducts induced by gamma radiation and their toxicity: the case of 2-nitrophenol," Environ. Technol., vol. 39, no. 8, pp.

967–976, 2018.
[17] N. Wang, G. Lv, L. He, and X. Sun, "New insight into photodegradation mechanisms, kinetics and health effects of p-nitrophenol by ozonation in polluted water," J. Hazard. Mater., vol. 403, p. 123805, 2021.
[18] X. Dang et al., "Sustainable electrochemical synthesis of natural starch-based biomass adsorbent with ultrahigh adsorption capacity for Cr (VI) and dyes removal," Sep. Purif. Technol., vol. 288, p. 120668, 2022.
[19] G. Wang, G. Gao, S. Yang, Z. Wang, P. Jin, and J. Wei, "Magnetic mesoporous carbon nanospheres from renewable plant phenol for efficient hexavalent chromium removal," Microporous Mesoporous Mater., vol. 310, p. 110623, 2021.
[20] "Enhancing chromium removal and recovery from industrial wastewater using sustainable and efficient nanomaterial: a review," Ecotoxicol. Environ. Saf., vol. 263, p. 115231, 2023.
[21] P. Kumari, M. Alam, and W. A. Siddiqi, "Usage of nanoparticles as adsorbents for waste water treatment: An emerging trend," Sustain. Mater. Technol., vol. 22, p. e00128, 2019.
[22] N. Ghosh, S. Das, G. Biswas, and P. K. Haldar, "Review on some metal oxide nanoparticles as effective adsorbent in wastewater treatment," Water Sci. Technol., vol. 85, no. 12, pp. 3370–3395, 2022.
[23] A. Roy, O. Bulut, S. Some, A. K. Mandal, and M. D. Yilmaz, "Green synthesis of silver nanoparticles: biomolecule-nanoparticle organizations targeting antimicrobial activity," RSC Adv., vol. 9, no. 5, pp. 2673–2702, 2019.
[24] M. Gonbadi, S. Sabbaghi, J. Rasouli, K. Rasouli, R. Saboori, and M. Narimani, "Green synthesis of ZnO nanoparticles for spent caustic recovery: Adsorbent characterization and process optimization using I-optimal method," Inorg. Chem. Commun., vol. 158, p. 111460, 2023.
[25] B. Dinesh, A. Bianco, and C. Ménard-Moyon, "Designing multimodal carbon nanotubes by covalent multi-functionalization," Nanoscale, vol. 8, no. 44, pp. 18596–18611, 2016.
[26] Y. Zhou, Y. Fang, and R. P. Ramasamy, "Non-covalent functionalization of carbon nanotubes for electrochemical biosensor development," Sensors, vol. 19, no. 2, p. 392, 2019.
[27] A. M. Awad et al., "Adsorption of organic pollutants by nanomaterial-based adsorbents: An overview," J. Mol. Liq., vol. 301, p. 112335, 2020.
[28] F. Mashkoor, A. Nasar, and Inamuddin, "Carbon nanotube-based adsorbents for the removal of dyes from waters: a review," Environ. Chem. Lett., vol. 18, pp. 605–629, 2020.
[29] Z. Fallah et al., "Toxicity and remediation of pharmaceuticals and pesticides using metal oxides and carbon nanomaterials," Chemosphere, vol. 275, p. 130055, 2021.
[30] A. A. Khan et al., "Metal oxide and carbon nanomaterial based membranes for reverse osmosis and membrane distillation: A comparative review," Environ. Res., vol. 202, p. 111716, 2021.
[31] U. Qumar et al., "Photocatalysis vs adsorption by metal oxide nanoparticles," J. Mater. Sci. Technol., vol. 131, pp. 122–166, 2022.
[32] H. A. Asmaly, N. Kabbashi, M. Z. Alam, and M. A. A. Yassin, "Capabilities of Novel Carbon Nano Adsorbents in Evaluating the Extraction of 2-Nitrophenol and Heavy Metal from Aqueous Solutions," Knowledge-Based Eng. Sci., vol. 4, no. 3, pp. 35–50, 2023.
[33] Z. Ciğeroğlu, G. Küçükyıldız, B. Erim, and E. Alp, "Easy preparation of magnetic nanoparticles-rGO-chitosan composite beads: Optimization study on cefixime removal based on RSM and ANN by using Genetic Algorithm Approach," J. Mol. Struct., vol. 1224, p. 129182, 2021.
[34] H. Karyab, M. Ghasemi, F. Ghotbinia, and N. Nazeri, "Efficiency of chitosan nanoparticle with polyaluminum chloride in dye removal from aqueous solutions: Optimization through response surface methodology (RSM) and central composite design (CCD)," Int. J. Biol. Macromol., vol. 249, p. 125977, 2023.
[35] T. M. Alslaibi, I. Abustan, M. A. Ahmad, and A. A. Foul, "Application of response surface

methodology (RSM) for optimization of Cu2+, Cd2+, Ni2+, Pb2+, Fe2+, and Zn2+ removal from aqueous solution using microwaved olive stone activated carbon," J. Chem. Technol. Biotechnol., vol. 88, no. 12, pp. 2141–2151, 2013.
[36] N. Resources and E. Journal, "The Effect of Acide modification on Adsorption of Ortho-Nitrophenol from aqueous solution by Multi wall Carbon Nanotubes: Characrization, Modification and Performance ," vol. 7, no. 1, 2023.
[37] A. A. Gouda and S. M. Al Ghannam, "Impregnated multiwalled carbon nanotubes as efficient sorbent for the solid phase extraction of trace amounts of heavy metal ions in food and water samples," Food Chem., vol. 202, pp. 409–416, 2016.
[38] L. Natrayan et al., "Synthesis and analysis of impregnation on activated carbon in multiwalled carbon nanotube for Cu adsorption from wastewater," Bioinorg. Chem. Appl., vol. 2022, 2022.
[39] T. A. Oyehan, T. Laoui, B. Tawabini, F. Patel, F. A. Olabemiwo, and M. A. Atieh, "Enhancing the adsorptive capacity of carbon nanofibers by impregnation with ferric oxide for the removal of cadmium from aqueous solution," J. Water Process Eng., vol. 42, p. 102130, 2021.
[40] Ihsanullah et al., "Effect of acid modification on adsorption of hexavalent chromium (Cr (VI)) from aqueous solution by activated carbon and carbon nanotubes," Desalin. Water Treat., vol. 57, no. 16, pp. 7232–7244, 2016.
[41] X. Zhao, F. Jiao, J. Yu, Y. Xi, and X. Jiang, "Colloids and Surfaces A: Physicochemical and Engineering Aspects Removal of Cu (II) from aqueous solutions by tartaric acid modified multi-walled carbon nanotubes," Colloids Surfaces A Physicochem. Eng. Asp., vol. 476, pp. 35–41, 2015, doi: 10.1016/j.colsurfa.2015.03.016.
[42] F. A. Al-Khaldi et al., "Adsorptive removal of cadmium (II) ions from liquid phase using acid modified carbon-based adsorbents," J. Mol. Liq., vol. 204, pp. 255–263, 2015.
[43] B. S. Brunauer and P. H. Emmett, "in Multimolecular," no. lc, 1938.
[44] S. Rio, C. Faur-Brasquet, L. Le Coq, P. Courcoux, and P. Le Cloirec, "Experimental design methodology for the preparation of carbonaceous sorbents from sewage sludge by chemical activation—application to air and water treatments," Chemosphere, vol. 58, no. 4, pp. 423–437, 2005.
[45] M. A. Bezerra, R. E. Santelli, E. P. Oliveira, L. S. Villar, and L. A. Escaleira, "Response surface methodology (RSM) as a tool for optimization in analytical chemistry," Talanta, vol. 76, no. 5, pp. 965–977, 2008.
[46] M. Aazza and H. Ahlafi, "Investigation of m-NP and p-NP adsorption from single and binary aqueous solutions onto Al2O3 and HDTMA+/Al2O3 composite using first derivative UV/Visible spectrophotometry," J. Mol. Liq., vol. 398, p. 124220, 2024.
[47] J. Zhou, Z. Zhang, B. Cheng, and J. Yu, "Glycine-assisted hydrothermal synthesis and adsorption properties of crosslinked porous -Fe2O3 nanomaterials for p-nitrophenol," Chem. Eng. J., vol. 211–212, pp. 153–160, 2012 doi: https://doi.org/10.1016/j.cej.2012.09.027.
[48] J. C. Lazo-Cannata et al., "Adsorption of phenol and nitrophenols by carbon nanospheres: Effect of pH and ionic strength," Sep. Purif. Technol., vol. 80, no. 2, pp. 217–224, 2011, doi: https://doi.org/10.1016/j.seppur.2011.04.029.
[49] G. Xue, M. Gao, Z. Gu, Z. Luo, and Z. Hu, "The removal of p-nitrophenol from aqueous solutions by adsorption using gemini surfactants modified montmorillonites," Chem. Eng. J., vol. 218, pp. 223–231, 2013, doi: https://doi.org/10.1016/j.cej.2012.12.045.
[50] B. Koubaissy, G. Joly, and P. Magnoux, "Present in Wastewater," pp. 9558–9565, 2008.
[51] E. Taghdir, M. Aghaie, and V. Hadadi, "Adsorption Study of Cr (III), Ni (II) and Zn (II) Ions onto the Multi Walledcarbon Nanotubes 1," vol. 9, no. 3, pp. 399–405, 2015, doi: 10.1134/S1990793115030100.
[52] F. Di Natale, A. Lancia, A. Molino, and D. Musmarra, "Removal of chromium ions form aqueous solutions by adsorption on activated carbon and char," J. Hazard. Mater., vol. 145, no. 3,

pp. 381–390, 2007, doi: https://doi.org/10.1016/j.jhazmat.2006.11.028.
[53] B. Dash, S. K. Jena, and S. S. Rath, "Adsorption of Cr (III) and Cr (VI) ions on muscovite mica: Experimental and molecular modeling studies," J. Mol. Liq., vol. 357, p. 119116, 2022, doi: https://doi.org/10.1016/j.molliq.2022.119116.
[54] J. Qiu, "Preparation of polyacrylamide – montmorillonite nanocomposite and its application in Cr (III) adsorption," no. June 2019, 2020, doi: 10.1002/app.49065.
[55] Rentsennorov U., Davaabal B., Dovchin B. and Temuujin J, "Adsorption of Cr(III) from aqueous media on zeolite A prepared from fused fly ash by hydrothermal synthesis," J. Ceram. Process. Res., vol.22,no .2,pp. 232–239,2021, doi.org/10.36410/jcpr.2021.22.2.232.
[56] Y Si, J Huo, Y Hengbo, A Wang, " Adsorption kinetics, isotherms, and thermodynamics of Cr (III), Pb (II), and Cu (II)on porous hydroxyapatite nanoparticles,".J.Nano.science and Nanotechnology.,vol.18,no.8,pp. 3484-3491 ,2018 ,doi.org/10.1166/jnn.2018.14631